

Dynamic prediction fatigue life of composite wind turbine blade

Samir Lecheb ^{*1}, Abdelkader Nour ¹, Ahmed Chellil ¹,
Hamza Mechakra ¹, Hicham Ghanem ¹ and Hocine Kebir ²

¹ *Laboratory of Engines Dynamics and Vibroacoustics, University of Boumerdes, Algeria*

² *Laboratory Roberval, University of Technology Compiègne, UTC, France*

(Received March 22, 2014, Revised October 30, 2014, Accepted November 02, 2014)

Abstract. In this paper we are particularly focusing on the dynamic crack fatigue life of a 25 m length wind turbine blade. The blade consists of composite materiel (glass/epoxy). This work consisted initially to make a theoretical study, the turbine blade is modeled as a Timoshenko rotating beam and the analytical formulation is obtained. After applying boundary condition and loads, we have studied the stress, strain and displacement in order to determine the critical zone, also show the six first modes shapes to the wind turbine blade. Secondly was addressed to study the crack initiation in critical zone which based to finite element to give the results, then follow the evolution of the displacement, strain, stress and first six naturals frequencies a function as crack growth. In the experimental part the laminate plate specimen with two layers is tested under cyclic load in fully reversible tensile at ratio test ($R = 0$), the fast fracture occur phenomenon and the fatigue life are presented, the fatigue testing exerted in INSTRON 8801 machine. Finally which allows the knowledge their effect on the fatigue life, this residual change of dynamic behavior parameters can be used to predicted a crack size and diagnostic of blade.

Keywords: wind turbine blade; composite material; dynamic fatigue life; crack growth

1. Introduction

Wind energy was one of the most ancient sources of energy used by mankind. HAWT have problems exploitation in near ground, more laminar wind stream. The rotor is composed of the hub and blades of the turbine. These components are often considered the largest sector in terms of improving the performance and cost effectiveness. Today most designs have three blades and some manufacturers have included the height monitoring of the pitch angle. Certain of intermediate size wind turbines have not fixed Manwell (2009). The turbine blades are made from composite materials, including fiber reinforced epoxy glass laminate. Charge is generated by aerodynamic lift and drag of the blade airfoil section, which depends on the wind speed, the speed of the blade surface, the angle of attack and yaw. The angle of attack depends on the torque of the blade pitch. The aerodynamic lift and drag are produced solved useful thrust in the direction of rotation and absorbed by the reaction force generator. We see that the reactive forces are significant action in the plane of bending wise flat and must be condoned by the blade with a

*Corresponding author, Ph.D., E-mail: samir_lecheb@yahoo.fr

restricted deformation Schubel and Crossley (2012). The blade is the most important component in a wind turbine which today is designed according to aerodynamic knowledge further developed to capture the maximum. Energy from the wind flow blades of horizontal axis are now all composite. Composites satisfy the constraints of complex design, such as minimal weight with sufficiently rigid while delivering good resistance to static load and fatigue Shokrieh and Rafiee (2006). In practice, the composite material is formed by the material of the assembly of two or more materials of different natures that have complementary properties, leading to a material which has properties of the better composite parts treated apart Berthelot (2006). The main requirements under wind turbine blades are: high strength to support extreme winds and the gravity load, high resistance to fatigue and fracture, high strength to ensure the stability of the optimal aerodynamic form and direction of the blade during work time and the gap between the blade and the tower, and low weight to reduce the load on the tower and the effect of centrifuge forces Mishnaevsky (2012). The Tsai-Wu criteria is a simplified theory of the general failure for orthotropic materials release. Assuming the existence of a fracture surface in the plane stress, a modified theory of polynomial tensor was put forward by Tsai and Wu, Isaac and Ori (1996). Similarly, (Reis *et al.* 2007, Thwe and Liao 2003, Ferreira *et al.* 2005) have characterized the SN curve of hybrid vegetable fiber composites / glass / polymer. Study of fatigue polypropylene / thermoplastic composite glass made from a bidirectional woven motley fabric of E-glass and polypropylene. This last is the matrix after the application of heat and pressure. This composite was fabricated with a volume fraction of 0.338. The effect of the design layer on the static and fatigue toughness was exploited. The results indicated, the fatigue strength was affected by the concept of the layer and the loss rigidity (E / E_o) began early in life fatigue, it can also noted linearly related between the loss of rigidity Ferreira *et al.* (1999a, b). Excellent syntheses bibliographic devoted on the developments of element-free in the analysis of composite structures, including static and dynamic analysis, free vibration Liew *et al.* (2011). The wind turbine blade is similar to a touchline. It is generally composed of more different profiles which are distributed along the span. The pitch angle shows the variation of the angle of attack of touchline assembly and the torque in the local change can be different for each aerofoil section. In this first part we defined the wind and its components; we also have recalls and setting air load, second reminder and definition associated with composite materials of the blade. Although more refined applications for composites fatigue material (Kensche 2006), Kong *et al.* 2006, Shokrieh and Rafiee 2006) are available. There are a (Baumgart 2002, Younsi *et al.* 2001) aimed mainly at modeling the mathematical dynamic behavior of the blade, investigated strain, natural frequencies, modes shapes, effect of dynamic response. Recently Liew and Uy (2001) devoted on composite frame design to obtained an idol design. Dynamic behavior used as indicator for prediction fatigue life by Lecheb *et al.* (2013). To study the statically and dynamical parts to modal analysis of a wind turbine blade, El Ghazly (1993) wrote a submission program using shell triangular finite elements type. Also, Younsi *et al.* (2001) devoted out a mathematical formulation to reduce the vibration of the blade structure. Murtagh *et al.* (2005) analyzed a free vibration of a HAWT blade rotation subjected to aerodynamic loading.

2. Mention equation modeling of the blade

Research for the vibratory characteristics of the revolving beams was studied. An very good examination of the topic can be described by (Leissa 1981, Rao and Gupta 2001). In fact, up to now, no analytical solution for the free vibration of a beam turning with an angle of inclination, in

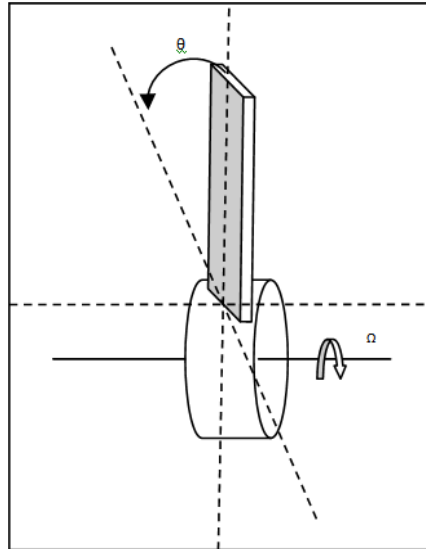


Fig. 1 Rotating beam with an angle of attack (θ)

which the effect of force of Coriolis and the deformation taken into account are presented Lin and Hsiao (2001) used the principle of Alembert to derive the equation of motion from a revolving beam of Timoshenko, and discussed the effect of coupling of the force of Coriolis and the deformation on the normal frequencies of a revolving beam. Lee and Sheu (2007) studied the effect of the force of Coriolis and the deformation on the normal frequencies of several qualitative relations between the normal frequencies and the physical parameters without numerical analysis. In this study, the theory used is the beam of Timoshenko. The dynamic analysis of a revolving beam with an angle of attack is led to include/understand the dynamic behavior of the blade.

Use a Hamilton's principle of the nonlinear beam theory. The motion equations of the rotating beam with an attack and inclination angles are derived as follows:

Displacements of the revolving beam in directions X , Y and Z can be expressed as is followed

$$\begin{aligned} u &= u_0(x,t) - z\psi(x,t) \\ v &= 0 \\ w &= w(x,t) \end{aligned} \tag{1}$$

Where u_0 is the field of displacement of the neutral axis of the beam in direction X , W is the field of displacement in the direction Z , ψ is the swing angle. Variable Z is the distance from a certain point P on an arbitrary section with the central axis, and T is the variable of time. The nonlinear normal deformation ε and the shearing strain γ are

$$\begin{aligned} \varepsilon &= \frac{\partial u_0}{\partial x} - z \frac{\partial \psi}{\partial x} + \frac{1}{2} \left(\frac{\partial w}{\partial x} \right)^2 \\ \gamma &= \frac{\partial w}{\partial x} - \psi \end{aligned} \tag{2}$$

The nonlinear normal stress σ and the shearing stress τ are

$$\begin{aligned}\sigma &= E \left[\frac{\partial u_0}{\partial x} - z \frac{\partial \psi}{\partial x} + \frac{1}{2} \left(\frac{\partial w}{\partial x} \right)^2 \right] \\ \tau &= G \left[\frac{\partial w}{\partial x} - \psi \right]\end{aligned}\quad (3)$$

Where E , and G are the Young modulus and the module shearing of the beam, respectively. The modulus of elasticity and the shear modulus are the equivalent ones derived from the composite material theory.

The potential energy is in the form

$$\begin{aligned}\bar{U} &= \int_v \left(\frac{1}{2} \sigma \varepsilon + \frac{1}{2} \tau \gamma \right) \\ &= \int_0^L \int_{-b/2}^{b/2} \int_{-h/2}^{h/2} \left(\frac{1}{2} E \varepsilon^2 \right) dz dy dx + \int_0^L \int_{-b/2}^{b/2} \int_{-h/2}^{h/2} \left(\frac{1}{2} k G \gamma^2 \right) dz dy dx\end{aligned}\quad (4)$$

Where K is the factor of correction of shearing, L is the length of the beam; b and h are the width and the thickness of the beam in the direction of Y and Z , respectively.

Multilayer Shell beam have a constant shear distribution across thickness. This causes a decrease in accuracy especially for sandwich structures. Our formulation must using shear correction factors. k depends on the geometry and the Poisson's ratio. For our case a rectangular section is used.

The vector of position of the point P to an arbitrary cross section of the beam turning, after deformation, can be expressed like

$$\vec{r} = [R_h + (x + u)]\vec{i} + [y \sin \theta - (z + w) \cos \theta]\vec{j} + [y \cos \theta + (z + w) \sin \theta]\vec{k}\quad (5)$$

Where X is the distance from point A of origin at the point P in the axial direction, I, J, and K are the unit vectors of the reference mark $X' Y' Z'$. Moreover, the velocity V of the point P is

$$\begin{aligned}\vec{V} &= [\dot{u} + \Omega y \cos \theta + \Omega(z + w) \sin \theta]\vec{i} + [-\dot{w} \cos \theta]\vec{j} \\ &\quad + [w \sin \theta - \Omega R - \Omega(x + u) - \Omega(z + w) \cos \theta]\vec{k}\end{aligned}\quad (6)$$

The kinetic energy T is given

$$\bar{T} = \frac{1}{2} \int_0^L \rho A (\vec{V} \cdot \vec{V}) dx\quad (7)$$

Where ρ , A are the unit density and the section respectively. Using the principle of Hamilton of the no linear theory of the beam

$$\int_{t_1}^{t_2} \delta(U - T) dt = 0\quad (8)$$

The equations of the motion of the revolving beam with an angle of inclination are derived as follows

$$\begin{aligned} \rho A \left[-2 \frac{\partial w}{\partial t} \Omega \sin \theta + u_0 \Omega^2 - \frac{\partial^2 u_0}{\partial t^2} \right] + \frac{\partial}{\partial x} \left(EA \frac{\partial u_0}{\partial x} \right) &= -(x + R) \rho A \Omega^2 \\ \rho A \left[-\psi \Omega^2 + \frac{\partial^2 \psi}{\partial t^2} \right] + \frac{\partial}{\partial x} \left(-EI \frac{\partial \psi}{\partial x} \right) - \left[kGA \left(\frac{\partial w}{\partial x} - \psi \right) \right] &= 0 \\ \rho A \left[2 \frac{\partial u_0}{\partial t} \Omega \sin \theta + w \Omega^2 \sin^2 \theta - \frac{\partial^2 w}{\partial t^2} \right] + \frac{\partial}{\partial x} \left(kGA \frac{\partial w}{\partial x} - \psi \right) + \frac{\partial}{\partial x} \left(N \frac{\partial w}{\partial x} \right) &= 0 \end{aligned} \tag{9}$$

Where I is the moment of inertia of surface, and $N = EA(\partial u_0 / \partial x)$ is the centrifugal stiffening force. The Coriolis forces in the axial directions $((x + R)\rho A \Omega^2)$, it is observed that on the left side of the first equation. The boundary conditions corresponding are

$$x = 0 : \begin{cases} u_0 = 0 \\ \psi = 0 \\ w = 0 \end{cases} \quad x = L : \begin{cases} EA \frac{\partial u_0}{\partial x} = 0 \\ EI \frac{\partial \psi}{\partial x} = 0 \\ kGA \left(\frac{\partial w}{\partial x} - \psi \right) = 0 \end{cases} \tag{10}$$

3. Numerical simulation of blade

In this part of work we will see the finite element model of composite wind turbine blade using Abaqus CAE software, a geometrical model was created based on cross section profiles of shell and spar using Solid-works software. In the meshing process, second order shell elements were employed. Which can give the distribution of stress and field of the displacement also we will see the deformation and modes of wind blade without crack / crack. In this research, a composite material used in the specimen is glass/Epoxy patch. The physical and mechanical properties of material selection part produced by Lecheb *et al.* (2014):

- 2 value of young modulus: $E_1 = 38,600 \text{ MPa}$ $E_2 = 8,270 \text{ MPa}$
- 3 value of shear modulus: $G_{12} = 4,140 \text{ MPa}$ $G_{23} = 4,140 \text{ MPa}$ $G_{13} = 4,140 \text{ MPa}$

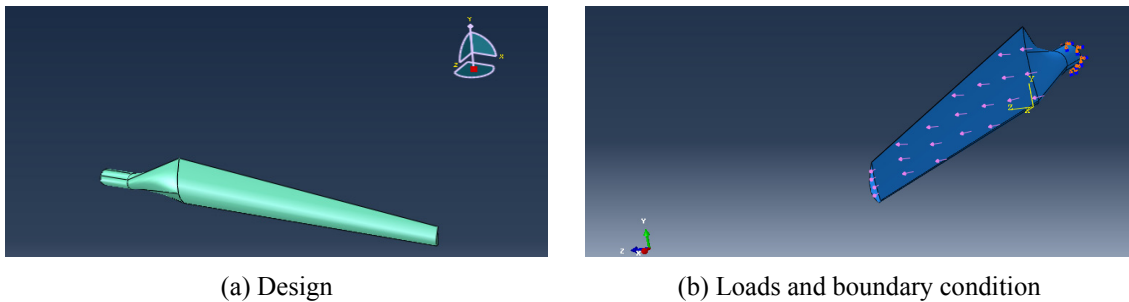


Fig. 2 Composite blade of wind turbine

- Density: 2.56 Kg/m³
- Poisson ratio: $\nu_{12} = 0.26$

In this part we create our blade geometry (area, volume, lines, key point) and then we create composite lamina with 2 plies with different's angles of fibers (0°/90°) in the progress of simulation we make different's numbers of ply with orientation of fibers.

A manual meshing method was employed. Therefore all elements have Tetrahedral shape with 6 nodes. The depiction of the FE model is shown in Fig. 2

Also in order to examine the case with both bending, torsion and tensile in the component, the loads (aerodynamic and centrifuge force) were applied and boundary conditions consisted of fixing all 6 degrees of freedom of nodes that are placed at the root. Model of wind blade turbine with loads and boundary condition shown in Fig. 2.

3.1 Convergence analysis

Convergence criteria should be considered to evaluate the results. Convergence analysis is performed on a composite model of the blade. By improving mesh density step-by-step a suitable number of elements is obtained. The stabilization of Von-Mises equivalent stress and natural frequencies shown in the figure below Chellil *et al.* (2013)

Shows the results of convergence analysis, it is clear that convergence is obtained with the use of about 20,000 or more elements.

3.2 Results

A mesh is an arrangement of finite elements defined on an FEA model. In ABAQUS/CAE we can define a mesh on a part or on the assembly. Meshing is the activity of discretizing geometry into a finite element representation. We use in this model the tetrahedral element to mesh all the part.

Table 1 Characteristic parameters of mesh refinement for convergence

Elements number	Nodes number	Total time [s] (2 plies)	Total time [s] (4 plies)
92154	46015	35.500	30.500
62894	31447	22.400	18.600
41218	20597	14.300	12.400
31946	15973	10.900	10.300
23886	11955	8.0000	6.9000
18134	9067	7.2000	5.1000
15102	7551	4.9000	4.3000
10848	5421	3.6000	3.2000
8120	4058	2.7000	2.4000
6470	3244	2.2000	2.0000
5310	2661	1.8000	1.6000
4490	2241	1.5000	1.4000

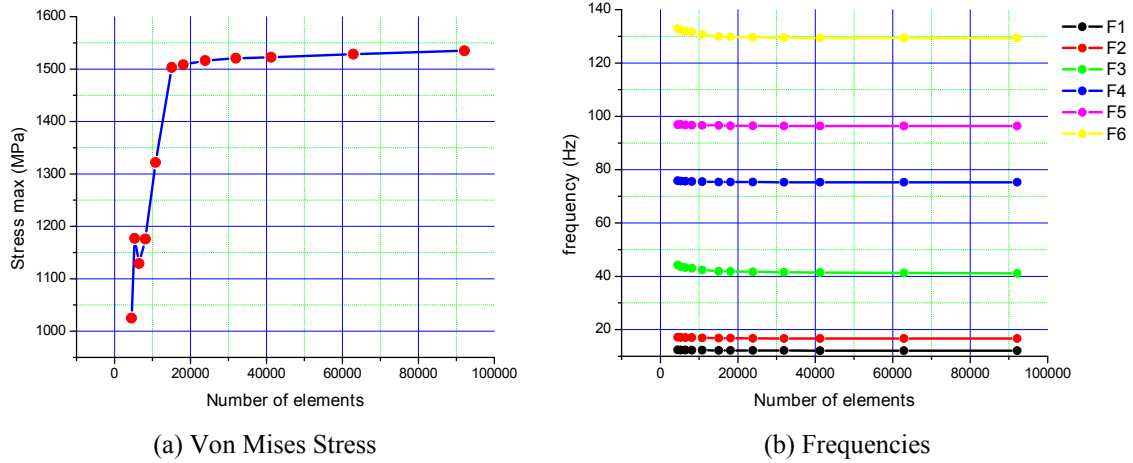


Fig. 3 Convergence based on Von Mises Stress and Six first frequencies (2 Plies)

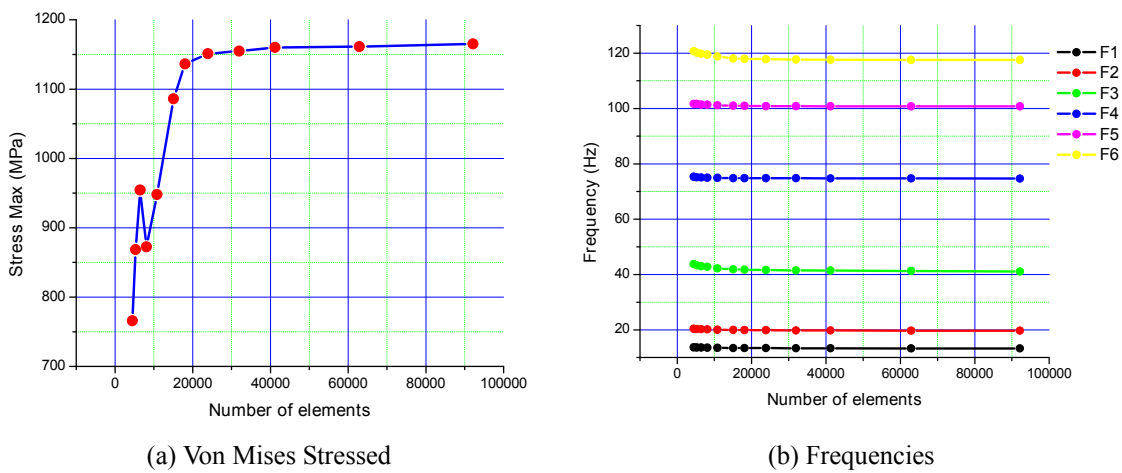


Fig. 4 Convergence based on Von Mises Stress and Six first frequencies (4 Plies)

Number of elements: 26,574

Number of nodes: 13,289

Von Mises stress

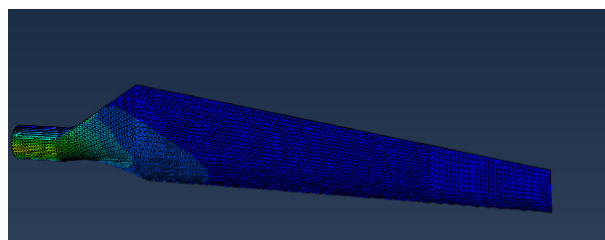
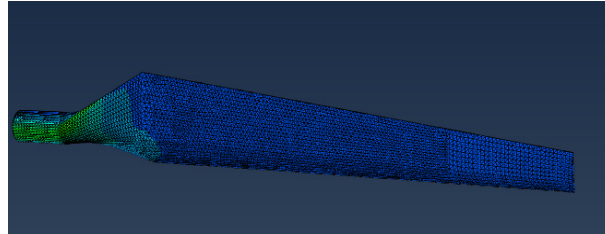
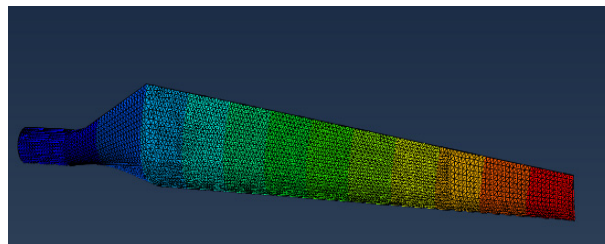


Fig. 5 Max Von Misses stress $S_{\max} = 1.417 \times 10^3$ Mpa

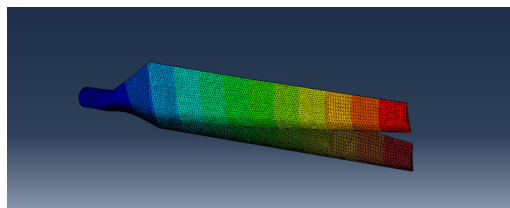
Strain

Fig. 6 Max Strain $E_{\max} = 6.104 \times 10^{-2d}$

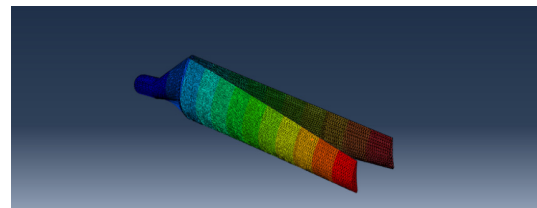
Displacement

Fig. 7 Max Displacement $U_{\max} = 2.514 \times 10^2$ mm

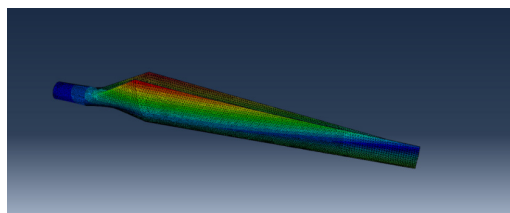
Six first modes shapes



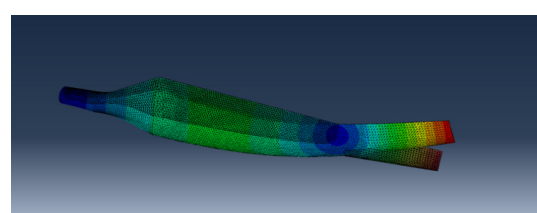
(a) First mode shape



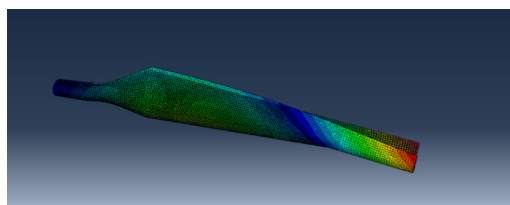
(b) Second mode shape



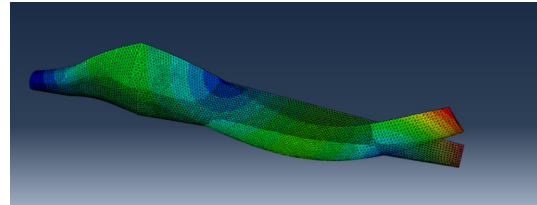
(c) Third mode shape



(d) Fourth mode shape



(e) Fifth mode shape



(f) Sixth mode shape

Fig. 8 First six modes shape of blade

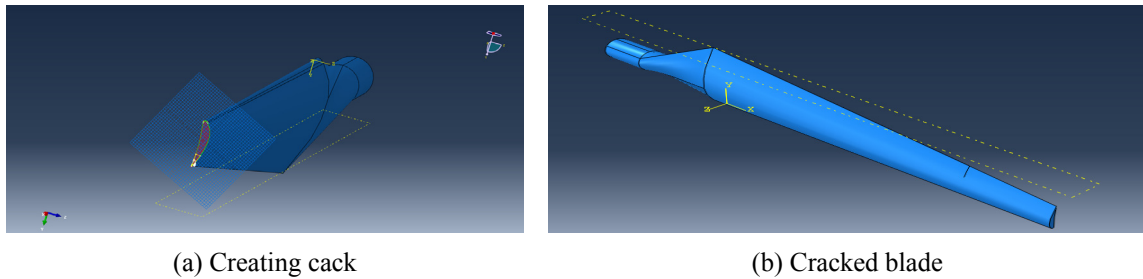


Fig. 9 Crack initiation of blade

3.3 Create model blade with crack

So, in this case we will create the same model but we will take into account the crack in the plate, the crack initiation is obtained by cut in the structure for type (crack seam) without removing material, the following fig show the cracked model.

In our simulation we impose a crack with deferent's length ($A = 10, 20, \dots, 60$ mm) in the same position and boundary condition, we use X-EFM method to solve problem of meshing and it has been used to crack propagation of specimen by method follows:

Code: ABAQUS/CAE.

Composite layup: layers number, thickness and rotation angle.

Mesh: Tri, Free.

Type: Crack seam.

Crack: Create Datum Plane Enter coordinate. Create Partition select datum plane and face of creating crack with position and then create form of Crack with length $A = 10$ as shown in Fig. 9.

We will do the same manipulation with the same boundary condition, Von Mises stress

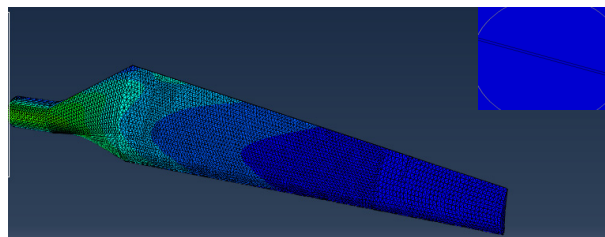


Fig. 10 Max Von Misses stress for cracked blade $S_{max} = 5.003 \times 10^3$ Mpa

Strain

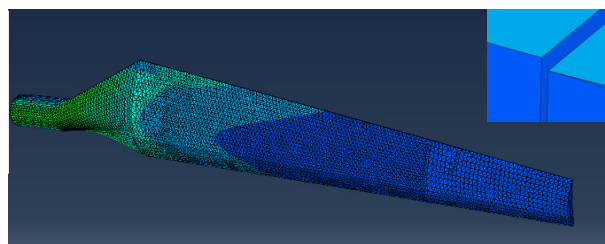


Fig. 11 Max deformation for cracked blade $E_{max} = 1.751 \text{ e-}01$

Displacement

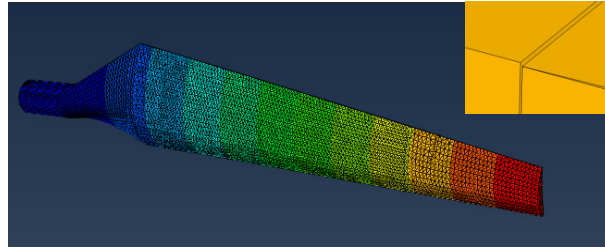


Fig. 12 Max displacement for cracked blade $U_{\max} = 4.351e + 3$ mm

Modes shapes of cracked blade (2 plies)

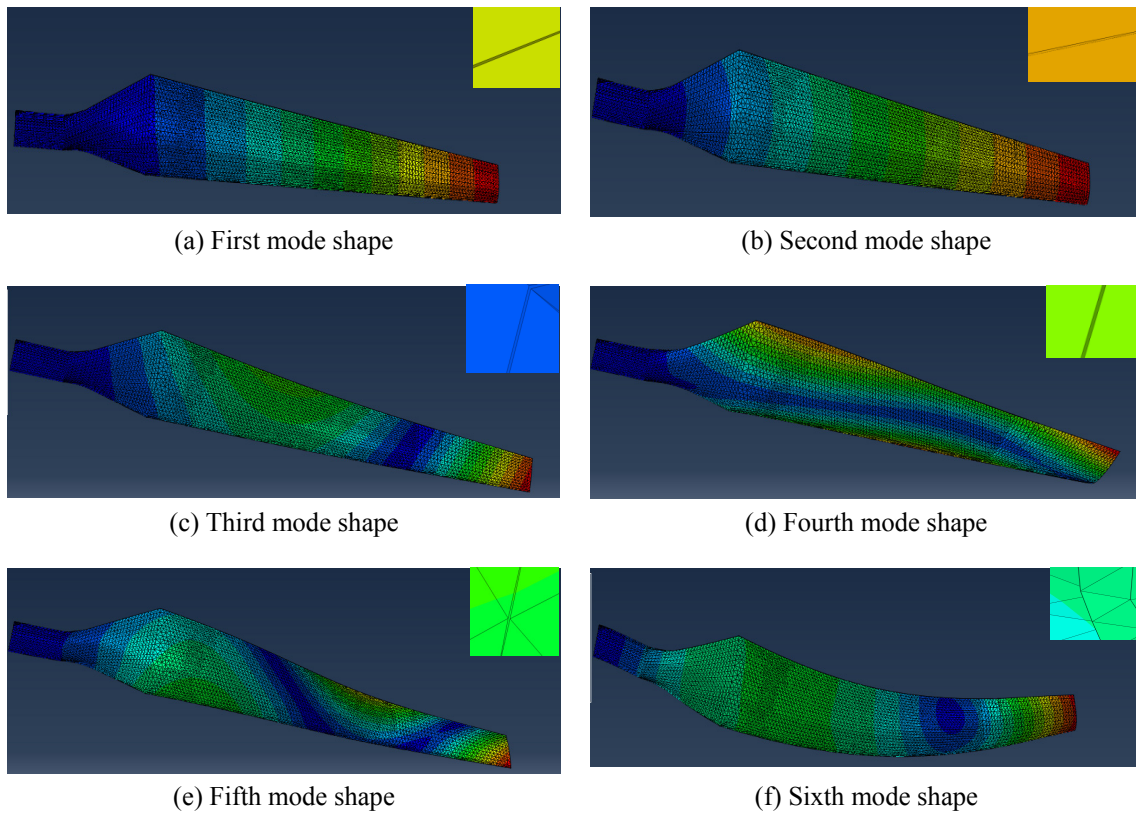


Fig. 13 First six modes shape of cracking blade

Create model blade with 4 plies: The same operation as 2 plies is executed.

3.4 Comparison and discussion

Comparison between blade before and after cracking

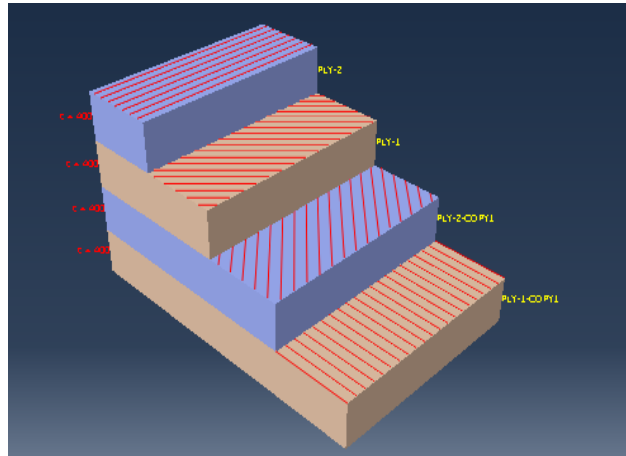


Fig. 14 Property of martial with 4 plies (0 -45 +45 0)

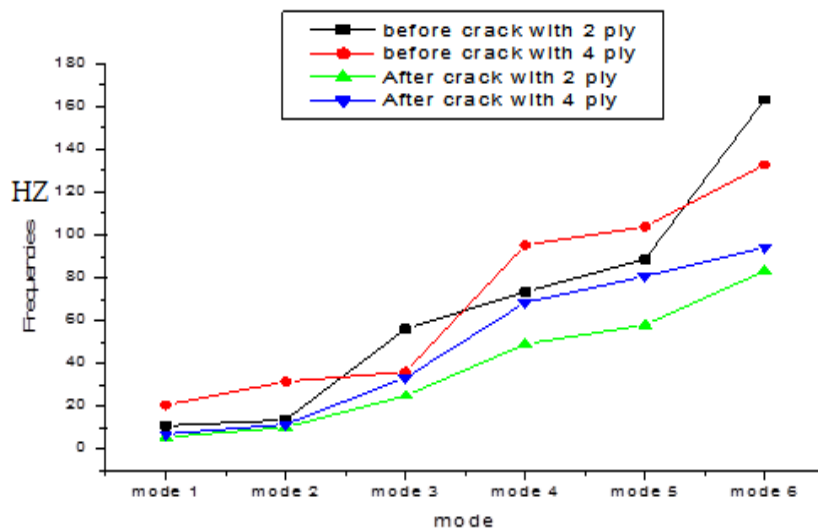


Fig. 15 Frequencies evaluation with mode of the blade before and after cracking

Table 2 Comparison of the maximum displacement before and after cracking

U_{MAX} (mm)	Before crack		After crack	
	2	4	2	4
Mode 1	1.039	1.019	1.002	1.002
Mode 2	1.040	1.031	1.010	1.008
Mode 3	1.002	1.000	1.000	1.000
Mode 4	1.030	1.031	1.001	1.004
Mode 5	1.001	1.017	1.000	1.000
Mode 6	1.105	1.001	1.033	1.031

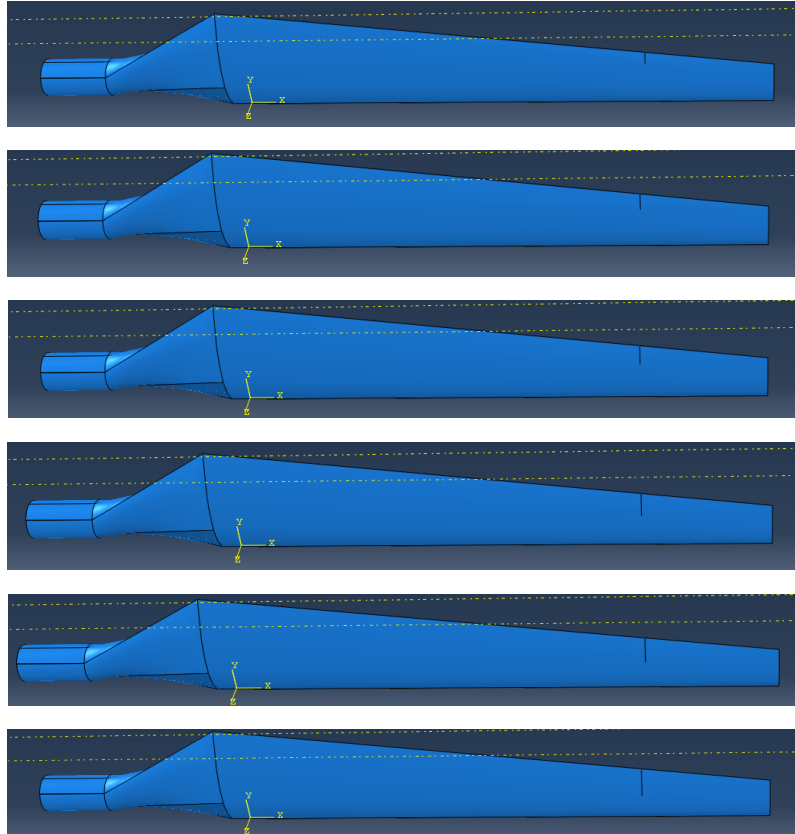


Fig. 16 Size of crack growth

We notice all natural frequencies increase after crack. The natural frequencies after cracking are decreases in a manner not linear.

Table 3 The frequencies in function of crack size

Crack size (mm)	F1 (Hz)		F2 (Hz)		F3 (Hz)		F4 (Hz)		F5 (Hz)		F6 (Hz)	
	2	4	2	4	2	4	2	4	2	4	2	4
$A_1 = 10$ mm	5.77	7.15	10.38	11.74	25.04	33.47	49.12	68.43	58.04	80.77	83.27	94.13
$A_2 = 20$ mm	5.75	7.01	10.36	11.67	24.99	32.52	49.01	66.58	57.93	78.23	83.17	93.92
$A_3 = 30$ mm	5.69	6.88	10.24	11.61	24.89	31.61	48.94	64.35	57.84	75.80	83.02	93.69
$A_4 = 40$ mm	5.67	6.75	10.15	11.53	24.78	30.74	48.89	61.46	57.75	73.42	82.86	93.42
$A_5 = 50$ mm	5.64	6.62	10.07	11.42	24.66	29.85	48.76	60.43	57.62	70.87	82.60	93.03
$A_6 = 60$ mm	5.53	6.47	9.99	11.23	24.54	28.75	48.67	59.41	57.58	67.41	82.32	92.32

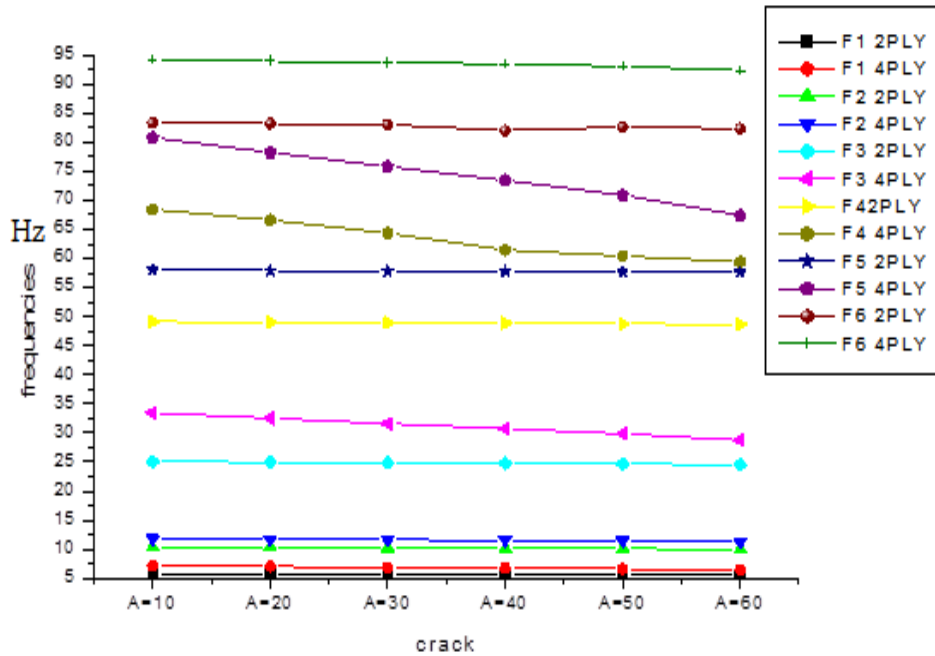


Fig. 17 Six first frequencies a function as crack size

Comparison of the maximum displacement before and after cracking:

3.5 Crack growth blade

In this case we introduce other frequencies with deferent crack size in Table 3.

In this case we have: the graphs of frequencies a function as crack size are nearly constant and we notice the frequencies with 4 ply are higher than 2 plies.

Table 4 Displacement, strain and Von Mises stress against crack size

Crack size (mm) A_x ply	V-mises (Mpa) $\times 10^{+03}$		Displacement (mm) $\times 10^{+03}$		Strain (E_{max}) $\times 10^{-01}$	
	2	4	2	4	2	4
$A_1 = 10$ mm	5.003	3.467	4.351	2.694	1.781	1.681
$A_2 = 20$ mm	5.057	3.543	4.946	3.679	1.793	1.742
$A_3 = 30$ mm	5.087	3.703	5.645	5.224	1.822	1.763
$A_4 = 40$ mm	5.154	3.915	6.472	7.829	1.836	1.772
$A_5 = 50$ mm	5.322	4.254	7.458	8.264	1.859	1.814
$A_6 = 60$ mm	5.530	4.641	8.646	9.751	1.874	1.836

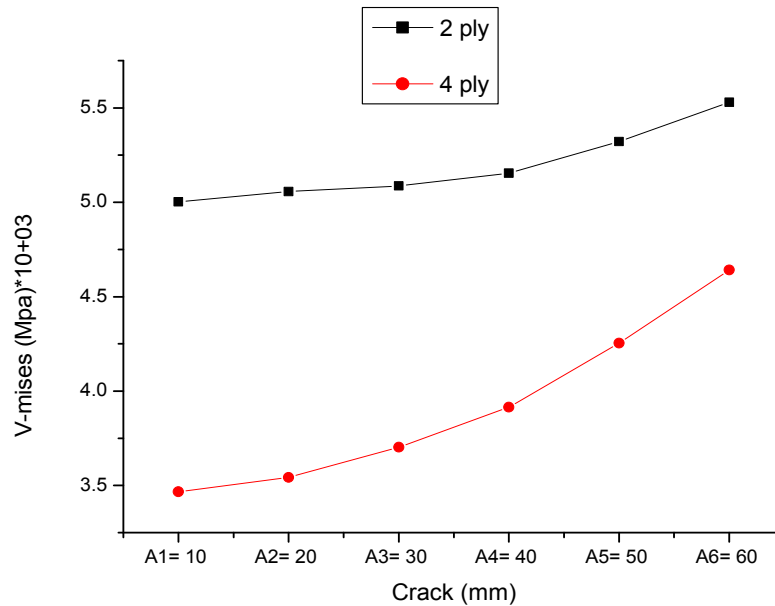


Fig. 18 Von Mises stress a function as crack size

We notice that when crack size increase the Von-mises stress increase in 2 case (2 plies end 4 plies).

We have the displacement are nearly constant with bouth (2 plies end 4 plies).

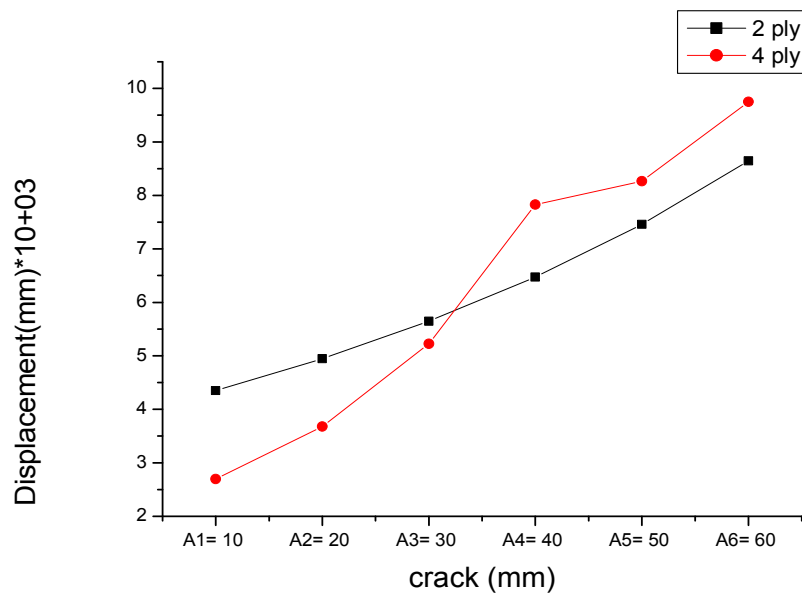


Fig. 19 Displacement against crack size

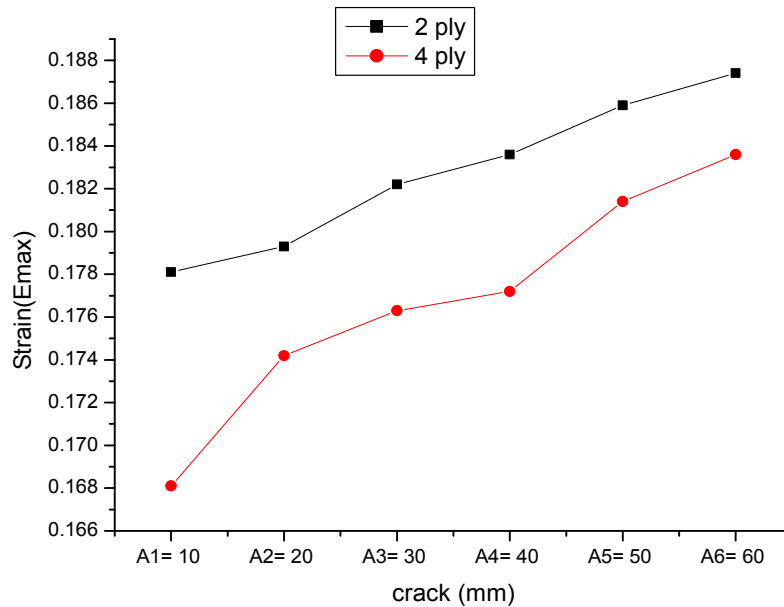


Fig. 20 Strain a function as crack size

We notice from the plot that the strain is increase with crack size.

4. Specimen test of blade and analysis of the crack growth

In this part we will see how we obtain the fatigue life of the specimen experimentally. So we speak about INSTRON 8801 machine, which can give us the variation of the strength, displacement and number of cycle. The specimen production process has been initiated with preparation of the test plates and the clamping plates. In total of two full scale (265×24.91 mm) GLASS/EPOXY plates had been produced to cover the full range of the test requirements. The plate was defined with average thickness of $e = 1.39$ mm and with two layers, and layup $[0/90]$. The specimen geometrical characteristics have been made according to ISO for composite laminate tension test. The objective of this experience is to determine the stress and strain to introduce the fatigue crack growth phenomenon. Sample tests are given by Ferreira, this geometry is used to provide a failure in the central part of the sample. As before, the samples are usually loaded from the load constant amplitude or displacement mode, Ferreira *et al.* (1999b).

Material properties:

The specimen has two continents; Fiberglass reinforcement epoxy.

Young modulus: $E_1 = 36,800$ MPa $E_2 = 8,270$ MPa

Shear modulus: $G_{12} = 4,041$ MPa $G_{13} = 4,041$ MPa $G_{23} = 4,041$ MPa

Poisson's ration: $\nu_{12} = 0.26$

$L = 265$ mm $B = 24.91$ mm 50% of matrix (resin) and 50% of fiber

Analyses and technical experience:

Force maximal $F_{max} = 2.5$ kN.

Force minimal $F_{min} = 0$ kN.

Stress Ratio test: $R = 0$.

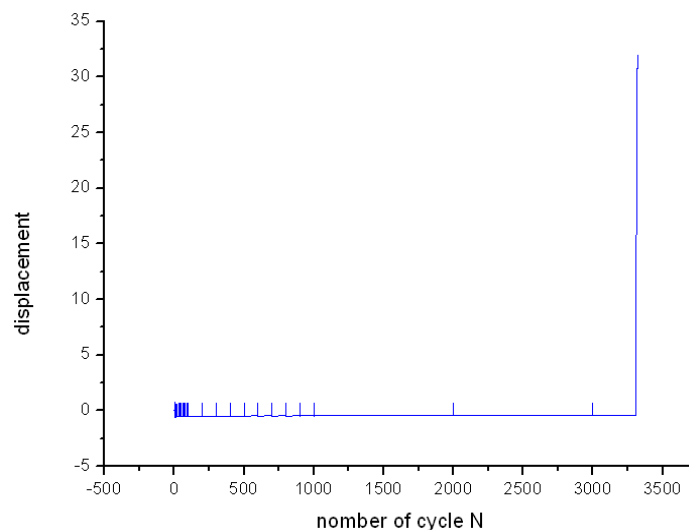
From the crack path of specimens, we find that the crack propagates perpendicular to the loading.

We see from the graph the reaction of fracture is happen in number of cycles 3310 and the fracture occurs. The displacement is constant until the fracture. We observe on figure, opening of the crack high, and then closing with a slow propagation to the sudden break of the specimen.

Therefore the effect of closure does not appear in our case, and the catastrophic fracture occurs.

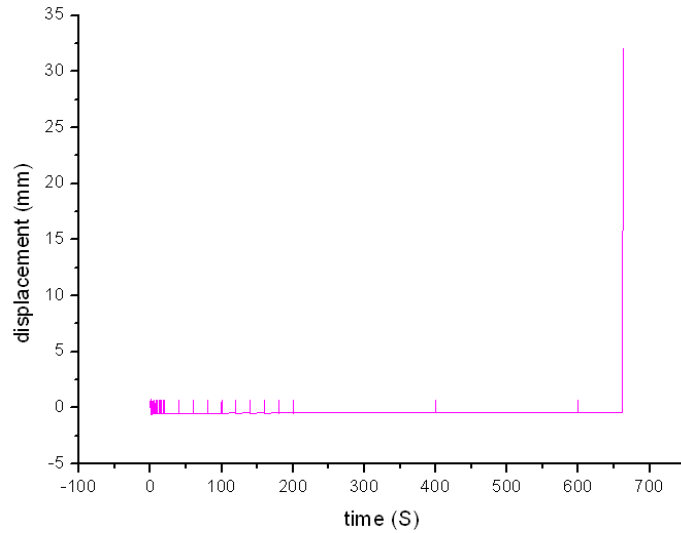


Fig. 21 Fracture of the specimen GLASS/EPOXY plat after 3310 cycles



(a) Cycles number

Fig. 22 Variation of the displacement a function as cycles number and time



(b) Time

Fig. 22 Continued

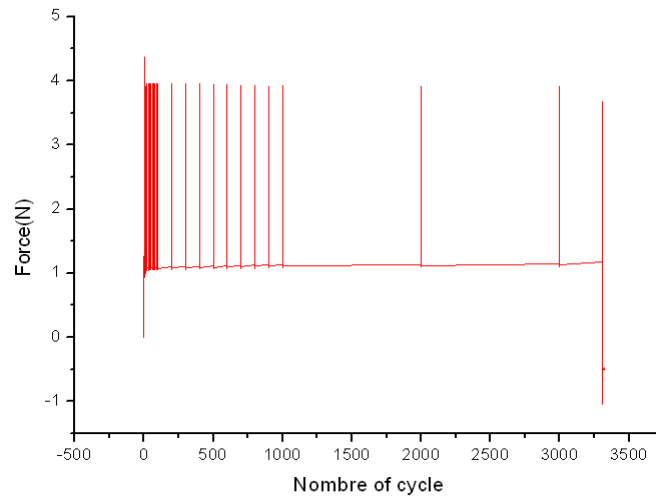


Fig. 23 Variation in the biasing force based on the number of cycle

5. Conclusions

In this current work based on modeling, finite element method, and test the tow case of wind blade composite by applying an aerodynamic force. The mention equation has obtained used Hamilton criteria, we calculates the frequencies and Eigen value, stress, strain and the displacement. After simulation we observed that frequencies in blade with (4 plies) are very high compared with the blade with (2 plies), and the value of strain, stress field displacement of the blade with (2 plies) in itself is also higher than the blade with (4 plies). as well as we noticed that

the blade without crack and with increasing crack size $a = (0 - 100)$ mm, the frequencies in the blade without crack are very high comparison with the blade with crack propagation in bouth (2 plies and 4 plies) and stress and displacement of the blade with crack are very large comparison with the blade without crack. Finally the natural frequencies decreases against crack growth because the natural frequency is related of rigidity (the stiffness of blade decrease and the mass is constant), but stress, strain, and displacement increases as function crack propagation. We see from the experience the fracture is occur after under 3310 cycles life, Therefore the effect of closure does not appear in our case, and the fracture brittle occur (fast fracture). The fracture in the composite materials occurs brittle.

References

- Baumgart, A. (2002), "A mathematical model for wind turbine blades", *J. Sound Vib.*, **251**(1), 1-12.
- Berthelot, J.M. (2006), *Matériaux Composites. Comportement mécanique et Analyse des structures*, (4th Ed.), Tech and Doc, France.
- Chellil, A., Nour, A., Lecheb, S., Kebir, H. and Chevalier, Y. (2013), "Impact of the fuselage damping characteristics and the blade rigidity on the stability of helicopter", *J. Aerosp. Sci. Technol.*, **29**(1), 235-252.
- El Ghazly, N.M. (1993), "Static and dynamic analysis of wind turbine blades using the finite element method", *Renew Energy*, **36**(16), 705-724.
- Ferreira, J.A.M., Costa, J.D.M. and Reis, P.N.B. (1999a), "Static and fatigue behavior of glass fiber reinforced polypropylene composites", *Theor. Appl. Fract. Mech.*, **31**(1), 67-74.
- Ferreira, J.A.M., Costa, J.D.M., Reis, P.N.B. and Richardson, M.O.W. (1999b), "Analysis of fatigue and damage in glass-fibre-reinforced polypropylene composite materials", *Compos. Sci. Technol.*, **59**(10), 1461-1467.
- Ferreira, J.M., Silva, H., Costa, J.D. and Richardson, M. (2005), "Stress analysis of lap joints involving natural fibre reinforced interface layers", *Compos.: Part B*, **36**(1), 1-7.
- Isaac, D. and Ori, I. (1996), *Engineering Mechanics of Composite Materials*, (2nd Edition), Oxford University Press, New York, NY, USA.
- Kensche, C.W. (2006), "Fatigue of composites for wind turbines", *Int. J. Fatigue*, **28**(10), 1363-1374.
- Kong, C., Kim, T., Han, D. and Sugiyama, Y. (2006), "Investigation of fatigue life for a medium scale composite wind turbine blade", *Int. J. Fatigue*, **28**(10), 1382-1388.
- Lecheb, S., Nour, A., Chellil, A., Sam, S., Belmiloud, D. and Kebir, H. (2013), "Prediction life of horizontal rotors by natural frequency evolution", *J. Des. Model. Mech. Syst.*, 105-110.
- Lecheb, S., Nour, A., Chellil, A., Mechakra, H., Amarache, A. and Kebir, H. (2014), "An advanced dynamic repair of edge crack aluminum plate with a composite patch", *Mater. Sci. Forum*, **794-796**, 716-721.
- Lee, S.Y. and Sheu, J. (2007), "Free vibration of an extensible rotating inclined Timoshenko beam", *J. Sound Vib.*, **304**(3-6), 606-624.
- Leissa, A. (1981), "Vibration aspects of rotating turbo machinery blades", *ASME Appl. Mech. Rev.*, **34**(5), 629-635.
- Liew, J.Y.R. and Uy, B. (2001), "Advanced analysis of composite frames", *Prog Struct Eng Mater*, **3**(2), 159-169.
- Liew, K.M., Zhao, X. and Ferreira, A.J.M. (2011), "A review of meshless methods for laminated and functionally graded plates and shells", *Compos. Struct.*, **93**(8), 2031-2041.
- Lin, S.C. and Hsiao, K.M. (2001), "Vibration analysis of a rotating Timoshenko beam", *J. Sound Vib.*, **240**(2), 303-322.
- Maalawi, K.Y. and Negm, H.M. (2002), "Optimal frequency design of wind turbine blades", *J. Wind Eng. Ind. Aerodyn.*, **90**(8), 961-986.
- Manwell, J.F. (2009), *Wind Energy Explained: Theory, Design and Application*, (2nd Ed.), John Wiley &

- Sons, West Sussex, UK.
- Mishnaevsky, J.R. (2012), "Composite materials for wind energy application", *Comput. Mech.*, **50**(2), 195-207.
- Murtagh, P.J., Basu, B. and Broderick, B.M. (2005), "Along wind response of a wind turbine tower with blade coupling subjected to rotationally sampled wind loading", *Eng. Struct.*, **27**(8), 1209-1219.
- Rao, S.S. and Gupta, R.S. (2001), "Finite element vibration analysis of rotating Timoshenko beams", *J. Sound Vib.*, **242**(1), 103-124.
- Reis, P.N.B., Ferreira, J.A.M., Antunes, F.V. and Costa, J.D.M. (2007), "Flexural behavior of hybrid laminated composites", *Compos.: Part A*, **38**(6), 1612-1620.
- Schubel, J.P and Crossley, R.J. (2012), "Wind turbine blade design", *MDPI Energ. J.*, **5**(9), 3425-3449.
- Shokrieh, M.M. and Rafiee, R. (2006), "Simulation of fatigue failure in a full composite wind turbine blade", *Compos. Struct.*, **74**(3), 332-342.
- Thwe, M.M. and Liao, K. (2003), "Durability of bamboo-glass fiber reinforced polymer matrix hybrid composites", *Compos. Sci. Technol.*, **63**(3-4), 375-387.
- Younsi, R., El-Batanony, I., Tritsch, J., Naji, H. and Landjerit, B. (2001), "Dynamic study of wind turbine blade with horizontal axis", *Eur. J. Mech. – A/Solids*, **20**(2), 241-252.

BU